The Hydrodynamics of Trickling Flow in Packed Beds

Part I: Conduit Models

The hydrodynamics of trickling flow in packed beds is modeled by representing the porous medium as an array of parallel conduits of circular cross section.

First, a straight tube model is developed and analytical solutions are obtained for the relative permeabilities of the gas and liquid phases. Then a periodically constricted tube model is proposed and the equations of motion are solved numerically to determine the effect that surface tension forces have on the relative permeabilities. The constricted tube model predicts that the relative permeabilities of the phases are appreciably sensitive to surface tension forces, a prediction that seems at odds with experimental observations. This discrepancy may be caused by the assumption of fully wetted surface area of particles employed in the model.

The straight tube model confirms experimental results indicating that the liquid phase relative permeability is, for practical purposes, insensitive to the gas flow rate and to the gas-to-liquid density and viscosity ratios. Both conduit models show that the gas phase relative permeability curves are strong functions of the gas phase Reynolds number when this parameter is small. For large gas Reynolds numbers, a single curve for the relative permeability as a function of saturation is obtained. These trends are observed in previous experimental studies.

A. E. Sáez and R. G. Carbonell
Department of Chemical Engineering
North Carolina State University
Raleigh, NC 27695

J. Levec
Department of Chemistry and Chemical Technology
Edvard Kardelj University
61000 Ljubljana, Yugoslavia

SCOPE

The steady downward flow of a gas and a liquid in a packed bed for low superficial velocities of both phases is termed the trickling flow regime; it occurs in a wide variety of practical applications. It is important to understand the hydrodynamics of these systems not only to design and operate the packed bed but also to help understand heat and mass transfer processes in trickle bed reactors.

The most important macroscopic hydrodynamic parameters for trickling flows in packed beds are the pressure drop and the liquid holdup. The current level of understanding of the hydrodynamics of these systems allows a prediction of these parameters by means of empirical correlations. So far, theoretical studies dealing with the hydrodynamics of the flow at the pore level have not been performed.

In this work we develop microscopic or pore level models that consider the flow of two phases through tubes under steady state conditions. First, the two-phase flow problem is solved in a straight tube. The simplicity of the straight tube geometry allows an analytical solution to the problem. The results are formu-

A. E. Sáez is currently at the Universidad Simon Bolivar, P.O. Box 80659, Caracas, Venezuela.

lated in terms of dimensionless groups that contain as a characteristic length the hydraulic diameter of the capillary so that the trends followed by the hydrodynamic parameters of the capillary tube can be compared to those of trickle beds.

A more complex model, consisting of a periodically constricted tube unit cell is then considered. The geometry of the constricted tube is chosen by equating the cross-sectional area variation of the tube with the flow area variation in a cubic array of spheres. The constricted tube model allows a study of the effect of surface tension forces on the hydrodynamics of the flow at the local level. In both the straight and constricted tube geometries we assume that the solid surfaces are fully wetted by the liquid. This is an assumption that does not fit in very well with the behavior of a real trickle bed reactor over some regimes of gas and liquid flow rates, as will be apparent in the second part of this paper.

The solution of the problems stated above provides information about the relative permeabilities of the gas and the liquid. These are macroscopic parameters that can be used to estimate the hydrodynamic performance of trickling flows, i.e., to predict pressure drops and liquid retentions. In Part II we present the results of experimental measurements of liquid holdups and gas phase pressure drops, and compare the predictions of these models to the experimentally observed relative permeabilities.

CONCLUSIONS AND SIGNIFICANCE

Two types of conduit models were constructed to study the hydrodynamics of trickling flows in packed beds. First, a one-dimensional straight tube model was developed and analytical expressions were derived for the gas and liquid relative permeabilities. A second model, consisting of a periodically constricted tube whose cross-sectional area variations corresponded to the variations in flow area in a cubic array of spheres, was then formulated. Relative permeabilities for the gas and the liquid were calculated from numerical solutions to the Navier-Stokes equations. The relative permeabilities can be used to predict the dynamic holdup and pressure drop in the packed bed.

The straight tube model shows that the liquid phase relative permeability curves are not sensitive to the Reynolds number of the gas phase, confirming previous experimental results. These curves are also insensitive to the gas-to-liquid viscosity and density ratios in the ranges usually observed in experimental studies.

The periodically constricted tube model yields an Ergun constant that is 20% lower than the experimental value corresponding to a cubic array of spheres and 8% lower than that of a random packing of the same porosity, indicating the suitability of the model for performing one-phase flow calculations. This model was used to study the effects of surface tension forces on relative permeabilities. It was found that the liquid phase relative permeabilities were very sensitive to the Eötvös number (ratio of gravitational to surface tension forces). These results contradict previous experimental observations, which lead to a unique representation for the liquid phase relative permeability in an ample range of Eötvös numbers. The large sensitivity exhibited by the model to surface tension forces is a result of the changes of the shape of the gas-liquid surface. It was observed that as the surface tension forces increase in magnitude, the gas-liquid interface becomes flatter and the symmetry of the configuration changes. In a real packed bed the partially dry areas and local instabilities at the phase interfaces tend to overshadow this predicted dependence.

The conduit models were also used to calculate gas phase relative permeabilities. It was found that for gas phase Reynolds numbers below a certain value, dependent on the liquid Reynolds number, the gas phase relative permeability-saturation curves were a strong function of the ratio of Reynolds to Galileo numbers of the gas. For large values of the gas phase Reynolds number all the relative permeability curves converge to a single function of saturation. This behavior is also observed experimentally in trickling flow through packed beds.

The gas phase relative permeability curves were also found to be very sensitive to the Eötvös number, according to the periodically constricted tube model. A more extensive experimental analysis is required in order to clarify the effects of surface tension forces.

The results obtained in this investigation show the convenience of using the relative permeability analysis in the study of trickling flow in packed beds. This analysis provides a simple way of obtaining the trends followed by macroscopic parameters from simple pore-scale models. A comparison of the theoretical results in this part of the paper with the experimental results shown in Part II indicates that even though there are some details of the role of surface tension forces that are not predicted accurately by the capillary and the periodically constricted tube models, many of the qualitative dependencies of relative permeabilities on saturation and gas and liquid Reynolds numbers are indeed observed experimentally. The failure of the models considered in this paper may be traced to the assumption of fully wetted solid surfaces that has been employed.

Introduction

The hydrodynamic behavior of cocurrent gas-liquid flows in packed beds has been traditionally studied from an empirical point of view. Our current level of understanding of this type of process is summarized in recent reviews of the literature (Gianetto et al., 1978; Shah, 1979; and Sáez, 1984). Previous investigators have stressed the prediction of pressure drop and liquid holdup by means of empirical correlations based on dimensional analysis and experimental observations over a relatively narrow range of experimental conditions. In a recent paper, Sáez and Carbonell (1985) have proposed a new approach for predicting these hydrodynamic parameters, using the concept of relative permeabilities. These investigators show that the macroscopic equations of motion for the liquid (β) and gas (γ) phases under trickling flow conditions can be expressed as

$$-\frac{d\langle P_\beta\rangle^\beta}{dx}+\rho_\beta g=\frac{1}{k_\beta}\left\{\frac{A\,Re_\beta^*}{Ga_\beta^*}+\frac{B\,Re_\beta^{*2}}{Ga_\beta^*}\right\}\rho_\beta g \tag{1}$$

$$-\frac{d\langle P_\gamma\rangle^\gamma}{dx}+\rho_\gamma g=\frac{1}{k_\gamma}\left\{\frac{A\,Re_\gamma^*}{Ga_\gamma^*}+\frac{B\,Re_\gamma^{*2}}{Ga_\gamma^*}\right\}\rho_\gamma g \tag{2}$$

In the equations above the definitions of the Reynolds and Galileo numbers are given by

$$Re_\alpha^*=\frac{\rho_\alpha\langle v_\alpha\rangle d_e}{\mu_\alpha(1-\epsilon)};\quad Ga_\alpha^*=\frac{\rho_\alpha^2 d_e^3 g\,\epsilon^3}{\mu_\alpha^2(1-\epsilon)^3}\qquad \alpha=\beta,\gamma$$

where $\langle v_\alpha\rangle$ is the superficial velocity of the α phase and d_e is the equivalent particle diameter ($6V_p/A_p$). The superficial velocity is nothing more than the volumetric flow rate of a given phase divided by the column area. It can be written in terms of the interstitial velocity u_α as ϵu_α where ϵ is the bed porosity. It can be seen from these equations that the relative permeabilities, k_β and k_γ, represent the ratio of the pressure drop in the bed under single-phase flow conditions, as predicted by the Ergun equation, to the pressure drop under two-phase flow conditions including the hydrostatic contributions.

In Eqs. 1 and 2, it has been assumed that the relative permeability of each phase is the same in the viscous and turbulent flow regimes. Sáez and Carbonell (1985) gathered experimental evidence to support this assertion.

When the pressure difference between gas and liquid phases is independent of axial position in the bed, Eqs. 1 and 2 can be subtracted to obtain

$$\frac{1}{k_\beta}\left\{\frac{A\,Re_\beta^*}{Ga_\beta^*}+\frac{B\,Re_\beta^{*2}}{Ga_\beta^*}\right\}-\frac{1}{k_\gamma}\left\{\frac{A\,Re_\gamma^*}{Ga_\gamma^*}+\frac{B\,Re_\gamma^{*2}}{Ga_\gamma^*}\right\}\frac{\rho_\gamma}{\rho_\beta}=1 \tag{3}$$

where we have considered that $\rho_\beta \gg \rho_\gamma$. This constraint will be satisfied by most gas-liquid systems.

If the dependence of the relative permeabilities on saturation is known, Eq. 3 provides the means of computing the liquid holdup for given values of the Reynolds and Galileo numbers for the two phases.

The dimensionless pressure drop per unit length, including gravitational contributions, is directly obtained from Eq. 2

$$\psi_\gamma=\frac{1}{k_\gamma}\left\{\frac{A\,Re_\gamma^*}{Ga_\gamma^*}+\frac{B\,Re_\gamma^{*2}}{Ga_\gamma^*}\right\} \tag{4}$$

A knowledge of the gas phase relative permeability as a function of the saturation allows an estimation of the pressure drop by means of Eq. 4. Sáez and Carbonell (1985) correlated the liquid phase relative permeability to the liquid phase reduced saturation, δ_β, defined by

$$\delta_\beta=\frac{\epsilon_\beta-\epsilon_\beta^0}{\epsilon-\epsilon_\beta^0} \tag{5}$$

They also correlated the gas phase relative permeability to the gas phase saturation, S_γ, given by the expression

$$S_\gamma=1-\frac{\epsilon_\beta}{\epsilon} \tag{6}$$

The correlations found can be summarized as follows:

$$k_\beta=\delta_\beta^{2.43} \tag{7}$$

$$k_\gamma=S_\gamma^{4.80} \tag{8}$$

Equation 7 was obtained from an analysis of 57 experimental data points of dynamic liquid holdup at zero gas flow rate for the air-water system. Equation 8 was the result of analyzing 17 data points for pressure drops at various liquid and gas flow rates obtained also with air and water as working fluids. These correlations were developed and tested in the following ranges of independent variables

$$5\le Re_\beta^*\le 1{,}500$$

$$5\le Re_\gamma^*\le 6{,}000$$

$$4\times 10^4\le Ga_\beta^*\le 1.3\times 10^8$$

$$150\le Ga_\gamma^*\le 5\times 10^5$$

This approach has the advantage that all of the information on flow rates, particle diameters, and physical properties of the fluids is contained in the equations of motion. A knowledge of the relative permeabilities as functions of saturation can allow accurate predictions for holdup and pressure drop for nearly all operating conditions in the trickling flow regime.

The work described above was based on a key assumption, namely, that the relative permeabilities were functions only of saturation. With the limited data available it was possible to justify such a supposition and obtain correlations that led to predictions of pressure drops to within 30% of experimental values and liquid holdups to within 15%. However, it is not clear that the relative permeabilities are going to be independent of surface tension (Eötvös numbers), liquid and gas phase Reynolds numbers, etc., over a very wide range of operating conditions. All effects of the solid packing are included in the definitions of the Reynolds and Galileo numbers. Using the above functions for relative permeabilities, Sáez and Carbonell were able to fit data for holdup and pressure drops in beds packed with Raschig rings, Berl saddles, spheres, cylinders, and carbon rings. This is a strong indication of the insensitivity of the relative permeability-saturation curves to the particle shape.

One of the objectives of this work is to learn more about the physics of two-phase flow in porous media and to determine the

expected dependence of relative permeabilities on system parameters by using some reasonable approximations to the flow geometry. This is achieved by solving the equations of motion and continuity for the case of two-phase flow in a geometry that, it is hoped, is representative of the local scale in the packed bed. The solution of the local problem allows a direct evaluation of the relative permeabilities and a complete study of all the factors that can influence these macroscopic quantities. The selection of a representative geometry is difficult since the real local geometry of a porous medium is too complex for analytical purposes. The simplest geometry that can be chosen is the straight capillary tube. The hydrodynamics of one-phase viscous flow in a capillary tube suggests a linear relationship between the flow rate and the pressure drop (Hagen-Poiseuille equation), which is precisely what is observed macroscopically in a porous medium as stated by Darcy's law. However, the prediction of permeabilities by using straight tube models is poor (Scheidegger, 1974). This failure leads to the introduction of additional parameters such as the tortuosity that give a semiempirical aspect to such models.

The straight tube models can be useful in the prediction of some parameters related to heat and mass transfer in one-phase flow through packed beds, as shown by Zanotti and Carbonell (1984). These investigators were able to predict thermal axial dispersion coefficients in packed beds by using a capillary tube model. Despite the fact that the results showed too strong a Péclet number dependence, they provided good physical insights for the analysis of the macroscopic phenomena. The comparisons made by Zanotti and Carbonell (1984) between capillary tubes and packed beds were based on the choice of the hydraulic diameter of each system as the appropriate length that characterizes the local scale.

The simplicity of straight tube models imposes strong constraints on their applicability. However, these models provide useful information regarding the trends followed by the macroscopic variables. For this reason, we have developed a capillary tube model as a first approximation to the study of cocurrent gas-liquid flows in packed beds.

The recent improvement of numerical techniques to solve fluid mechanics and transport phenomena problems allows the treatment of more complex and realistic geometries. The actual trend in the modeling of porous media processes calls for two- and three-dimensional representations of the pore level structure. These models are generally based on the idea of spatial periodicity: the porous medium is conceptualized as being made up of geometrical units, termed unit cells, that exhibit translational symmetry (Brenner, 1980; Carbonell and Whitaker, 1984). A specific geometry is proposed for the unit cell and the fundamental equations describing the process to be studied are solved in this domain by including the symmetry provided by the periodicity of the geometry. The macroscopic parameters are then evaluated from the local solution by means of spatial averaging techniques.

A two-dimensional, spatially periodic model was develoed by Eidsath et al. (1983) to study hydrodynamics and dispersion in one-phase flow through packed beds. A full three-dimensional approach was followed by Sørensen and Stewart (1974a,b). These investigators studied fluid flow and heat and mass transfer phenomena in a cubic array of spheres. More recently, Zick and Homsy (1982) solved the hydrodynamics of one-phase flow through arrays of spheres for various spatial arrangements.

The spatially periodic models mentioned above are sometimes classified as external flow models because the geometrical description used resembles the structure of the packing particles. When the geometry of the unit cell is chosen to be a representation of the structure of the pore, the model is termed an internal flow model. The capillary tube models can be classified in this category. One of the most widely used models in the analysis of porous media processes belongs to the internal flow type. We are referring to the periodically constricted tube model, in which the unit cell is conceived as a tube with converging and diverging sections.

The periodically constricted tube model was first studied extensively by Payatakes et al. (1973). These investigators solved the hydrodynamic problem of one-phase flow through a unit cell whose geometrical characteristics were found by means of a statistical analysis based on experimental capillary pressure data. A good agreement was found in the prediction of friction factor-Reynolds number curves. That model was later extended to take into account random orientation of the pore structure by Payatakes and Neira (1977). Neira and Payatakes (1978, 1979) studied one-phase flow through periodically constricted tubes with various wall profiles, including parabolic and sinusoidal tubes. A wall profile consisting of step changes in diameter was considered by Azzam and Dullien (1977). Deiber and Schowalter (1979) studied the case of one-phase flow through sinusoidal tubes theoretically and experimentally.

The applications of the periodically constricted tube model to transport processes in one-phase flow through porous media have recently been reviewed by Pendse et al. (1983). So far, this type of model has been applied to processes involving the flow of one phase only. In the present work we are concerned with the use of periodically constricted tubes to model two-phase flow hydrodynamics in packed beds. In a recent work, Dassori et al. (1984) solved the related problem of viscous two-phase flow through a sinusoidal channel by means of a regular perturbation analysis, valid for small amplitudes of the wall oscillations. In the present work we study the application of the perodically constricted tube model to the simulation of trickle bed hydrodynamics.

Theoretical Aspects

One of the objectives of this work is to obtain the relative permeability of each phase as a function of the independent parameters characterizing the flow through the porous medium. The relative permeability is defined as the ratio of the one-phase flow pressure drop (including gravitational contributions) to the two-phase flow pressure drop obtained at the same interstitial velocity

$$k_\alpha = \frac{\psi_\alpha^{(1)}}{\psi_\alpha}, \qquad \alpha = \beta,\gamma \tag{9}$$

where $\psi_\alpha^{(1)}$ and ψ_α are the dimensionless pressure drops of phase α, measured in the direction of mean flow. We have assumed that the macroscopic flow is one-dimensional. In the present work, we will obtain the relative permeabilities of gas and liquid phases flowing through a tube with a periodic wall profile. According to Eq. 9, we need to estimate both the one-phase and the two-phase pressure drops.

One-phase flow through a tube with periodic wall profile

Consider a periodically constricted tube consisting of the repetition along the x axis of the unit cell structure shown in Figure 1. The periodicity of the wall profile can be expressed as

$$r'_\sigma(x') = r'_\sigma(x' \pm n\ell) \quad n = 0, 1, \ldots \tag{10}$$

The analysis is limited by the following assumptions:

1. The flow is laminar and steady.
2. The flow is axisymmetric.
3. The flow is incompressible.
4. The Reynolds numbers are low (negligible inertial effects).
5. The fluid is Newtonian.

Using these approximations, the continuity and momentum equations can be expressed as follows

$$\nabla' \cdot \boldsymbol{v}' = 0 \tag{11}$$

$$0 = -\nabla' P' + \rho \boldsymbol{g} + \nabla' \cdot \boldsymbol{\tau}' \tag{12}$$

where the primes denote dimensional quantities. The stress tensor, $\boldsymbol{\tau}'$, is given by

$$\boldsymbol{\tau}' = \mu[\nabla' \boldsymbol{v}' + (\nabla' \boldsymbol{v}')^T] \tag{13}$$

The boundary conditions are

1. No slip at the wall

$$\boldsymbol{v}' = 0 \quad \text{at } r' = r'_\sigma(x') \tag{14}$$

2. Symmetry about $r' = 0$

$$\frac{\partial v'}{\partial r'} = 0 \quad \text{at } r' = 0 \tag{15}$$

3. Spatial periodicity of the surface (Eq. 10)

The set of equations and boundary conditions stated above is invariant to a coordinate transformation of the form

$$x' \xrightarrow{T(x')} x' \pm n\ell, \qquad n = 0, 1, \ldots$$

Therefore, the solution to the set of equations can be proved to exhibit spatial periodicity, so that

$$\boldsymbol{v}'(x') = \boldsymbol{v}'(x' \pm n\ell) \tag{16}$$

$$\nabla' P'(x') = \nabla' P'(x' \pm n\ell) \tag{17}$$

It can be proved (Sáez, 1984) that the pressure can be decomposed into the sum of a periodic contribution and a linear contribution as follows

$$P' = \hat{P}' + \frac{\Delta \bar{P} x'}{\ell} \tag{18}$$

where $\hat{P}'$ is periodic

$$\hat{P}'(x') = \hat{P}'(x' \pm n\ell) \tag{19}$$

and $\Delta \bar{P}$ is the area-averaged pressure drop through the unit cell,

$$\Delta \bar{P} = \bar{P}(x' + \ell) - \bar{P}(x') \tag{20}$$

The area-averaged pressure is defined as

$$\bar{P}(x') = \frac{1}{A_T} \int_{A_T} P' dA \tag{21}$$

where $A_T(x')$ is the local cross-sectional area of the tube. Note that P' and $\hat{P}'$ are functions of r, but $\bar{P}$ is a function of x' only. According to this decomposition, Eq. 12 becomes

$$0 = -\nabla' \hat{P}' - \frac{\Delta \mathcal{P}'}{\ell} \boldsymbol{e}_x + \nabla' \cdot \boldsymbol{\tau}' \tag{22}$$

where

$$\frac{\Delta \mathcal{P}'}{\ell} = \frac{\Delta \bar{P}}{\ell} - \rho g \tag{23}$$

We now proceed to make the basic equations dimensionless. Let us define the following dimensionless parameters:

$$x = x'/\ell \tag{24}$$

$$r = r'/\ell \tag{25}$$

$$\hat{P} = \hat{P}'/(-\Delta \mathcal{P}') \tag{26}$$

$$\boldsymbol{v} = \mu \boldsymbol{v}'/(-\ell \Delta \mathcal{P}') \tag{27}$$

By using these definitions, the problem can be stated in the following dimensionless form

$$\nabla \cdot \boldsymbol{v} = 0 \tag{28}$$

$$0 = -\nabla \hat{P} + \nabla \cdot \boldsymbol{\tau} + \boldsymbol{e}_x \tag{29}$$

$$\boldsymbol{\tau} = \nabla \boldsymbol{v} + (\nabla \boldsymbol{v})^T \tag{30}$$

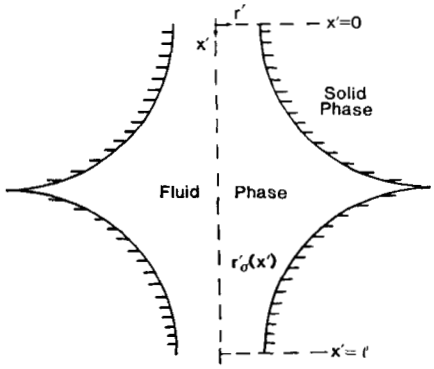

Figure 1. Periodically constructed tube, unit cell.

with boundary conditions

$$\boldsymbol{v} = 0 \quad \text{at } r = r_\sigma(x) \tag{31}$$

$$\frac{\partial \boldsymbol{v}}{\partial r} = 0 \quad \text{at } r = 0 \tag{32}$$

$$\boldsymbol{v}(x) = \boldsymbol{v}(x \pm n) \tag{33}$$

$$\hat{P}(x) = \hat{P}(x \pm n) \tag{34}$$

It can be proved that this problem has a unique solution for the velocity field as well as a unique solution up to an arbitrary constant for the periodic part of the pressure field (Sáez, 1984). Furthermore, the basic equations show that the solutions for $\boldsymbol{v}$ and $\hat{P}$ are only functions of the geometry of the unit cell, namely, $r_\sigma(x)$.

The dimensionless pressure drop, ψ, is defined by

$$\psi = -\frac{\Delta \mathcal{P}'}{\rho g \ell} \tag{35}$$

and the interstitial velocity is given by

$$\boldsymbol{u} = \frac{1}{V}\int_V \boldsymbol{v}'\, dV \tag{36}$$

where V is the volume of fluid in a unit cell of conduit. This is simply the average fluid velocity in the conduit. If we write Eq. 27 for the component of the flow in the direction of the axis of the conduit, and take the average over the fluid volume in the unit cell of the constricted tube we obtain

$$\frac{1}{V}\int_V v_x dV = -\frac{\mu}{\ell \Delta \mathcal{P}'}\frac{1}{V}\int_V v_x'\, dV \tag{37}$$

Now we let u be the magnitude of $\boldsymbol{u}$ along the x direction and use Eq. 35 to write

$$\psi = \frac{1}{\frac{1}{V}\int_V v_x dV}\frac{\mu u}{\rho g \ell^2} \tag{38}$$

This is the relation between the dimensionless mean pressure drop in the tube to the average fluid velocity. We can write this equation in terms of the Galileo and Reynolds numbers, using as a characteristic length the hydraulic diameter, defined as

$$d_h' = \frac{6V}{A_w} \tag{39}$$

where A_w is the wetted area of conduit and V is the fluid volume. The Reynolds and Galileo numbers then become

$$Re^* = \frac{\rho u d_h'}{\mu}; \qquad Ga^* = \frac{\rho^2 g d_h'^3}{\mu^2} \tag{40}$$

If we multiply the numerator and denominator of Eq. 38 by $d_h'^2$ and rearrange terms we obtain

$$\psi = A\frac{Re^*}{Ga^*} \tag{41}$$

where

$$A = \frac{d_h'^2/\ell^2}{\frac{1}{V}\int_V v_x dV} \tag{42}$$

Obviously, Eq. 41 is in the form of the Ergun equation when viscous effects dominate, and A is the Ergun constant. From Eqs. 28–34 we seen that v_x only depends on the shape chosen for the conduit, $r_\sigma(x)$. Similarly, the hydraulic diameter is also calculable directly from $R_\sigma(x)$; in fact, the relation is

$$d_h = \frac{d_h'}{\ell} = \frac{3\int_0^1 r_\sigma^2(x)dx}{\int_0^1 r_\sigma(x)\sqrt{1+\left(\frac{dr_\sigma}{dx}\right)^2}dx} \tag{43}$$

Thus, from the solution for v_x for a given $r_\sigma(x)$ one can get the value of the Ergun constant A in Eq. 42. This value can be directly compared to the Ergun constant in a packed bed since the definitions of the Reynolds and Galileo numbers in Eq. 40 are consistent with those used in Eq. 1. For instance, in a packed bed the fluid volume is related to the volume of particles by the ratio $\epsilon/(1-\epsilon)$. As a result, Eq. 39 can be written as

$$d_h' = d_e\left(\frac{\epsilon}{1-\epsilon}\right)$$

Substituting into Eq. 40 and writing the interstitial velocity of the fluid in the packed bed as $u = \langle v \rangle/\epsilon$ we obtain

$$Re^* = \frac{\rho\langle v\rangle d_e}{\mu(1-\epsilon)}; \qquad Ga^* = \frac{\rho^2 g d_e^3}{\mu^2}\frac{\epsilon^3}{(1-\epsilon)^3}$$

Of course, these are the same definitions of the Reynolds and Galileo numbers used in Eq. 1.

Two-phase flow through a tube with periodic wall profile

Let us consider now the case of two-phase flow through a periodically constricted tube, Figure 2. In addition to the assumptions listed in the previous section, we will suppose that the liquid phase is flowing in axisymmetric fashion along the wall of the tube and that surface tension gradients along the gas-liquid interface are negligible. Under these conditions, the differential equations and boundary conditions governing the hydrodynamics of both phases are given in dimensionless form by

Continuity equations

$$\nabla \cdot \boldsymbol{v}_\beta = 0 \quad r_\beta \le r \le r_\sigma \tag{44}$$

$$\nabla \cdot \boldsymbol{v}_\gamma = 0 \quad 0 \le r \le r_\beta \tag{45}$$

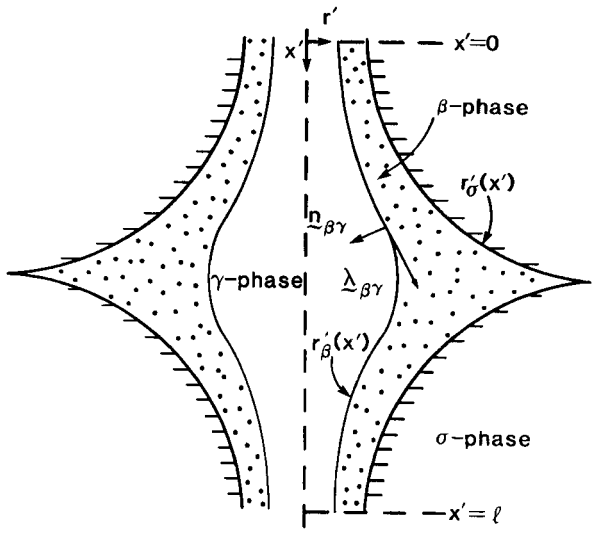

Figure 2. Periodically constricted tube, unit cell, two fluid phases.

Momentum equations

$$-\nabla P_\beta + e_x + \nabla \cdot \tau_\beta = 0 \quad r_\beta \le r \le r_\sigma \tag{46}$$

$$-\nabla P_\gamma + e_x + \nabla \cdot \tau_\gamma = 0 \quad 0 \le r \le r_\beta \tag{47}$$

Boundary conditions

No slip

$$v_\beta = 0 \quad \text{at } r = r_\sigma \tag{48}$$

Continuity of tangential velocity components at the gas-liquid interface

$$(\omega/\xi) v_\beta \cdot \lambda_{\beta\gamma} = v_\gamma \cdot \lambda_{\beta\gamma} \quad \text{at } r = r_\beta \tag{49}$$

Symmetry at the center of the cell

$$\frac{\partial v_\gamma}{\partial r} = 0 \quad \text{at } r = 0 \tag{50}$$

No mass transfer between phases implies

$$v_\beta \cdot n_{\beta\gamma} = 0 \quad \text{at } r = r_\beta \tag{51}$$

$$v_\gamma \cdot n_{\beta\gamma} = 0 \quad \text{at } r = r_\beta \tag{52}$$

Continuity of the stress vector at the gas-liquid interface gives

$$\left(P_\beta + \frac{2H}{E\ddot{o}}\right) n_{\beta\gamma} - \tau_\beta \cdot n_{\beta\gamma} = \xi(P_\gamma n_{\beta\gamma} - \tau_\gamma \cdot n_{\beta\gamma}) \quad \text{at } r = r_\beta \tag{53}$$

In these equations, the dimensionless variables have been defined using the relations

$$x = x'/\ell \tag{54}$$

$$r = r'/\ell \tag{55}$$

$$v_\alpha = \frac{\mu_\alpha}{\ell^2 \rho_\alpha g} v'_\alpha, \quad \alpha = \beta,\gamma \tag{56}$$

$$P_\alpha = \frac{P'_\alpha}{\rho_\alpha g \ell}, \quad \alpha = \beta,\gamma \tag{57}$$

$$\xi = \rho_\gamma/\rho_\beta \tag{58}$$

$$\omega = \mu_\gamma/\mu_\beta \tag{59}$$

and

$$E\ddot{o} = \frac{\rho_\beta g \ell^2}{\sigma} \tag{60}$$

Note that the velocity and pressure have been made dimensionless using different characteristic quantities from those used in the one-phase flow formulation.

The dimensionless mean curvature, H, is given by (Adamson, 1976, Ch. I)

$$H = \frac{1}{2}\left(\frac{1}{r_s} + \frac{1}{r_c}\right) \tag{61}$$

where

$$r_c = \frac{-\left[1 + \left(\frac{dr_\beta}{dx}\right)^2\right]^{3/2}}{\frac{d^2 r_\beta}{dx^2}} \tag{62}$$

and

$$r_s = r_\beta \sqrt{1 + \left(\frac{dr_\beta}{dx}\right)^2} \tag{63}$$

The normal and tangent unit vectors can be expressed as functions of dr_β/dx by the relations

$$n_{\beta\gamma} = \frac{1}{\sqrt{1 + \left(\frac{dr_\beta}{dx}\right)^2}}\left(-e_r + \frac{dr_\beta}{dx} e_x\right) \tag{64}$$

and

$$\lambda_{\beta\lambda} = \frac{1}{\sqrt{1 + \left(\frac{dr_\beta}{dx}\right)^2}}\left(\frac{dr_\beta}{dx} e_r + e_x\right) \tag{65}$$

In addition to these equations, the pressure of each phase can be decomposed into a periodic and a macroscopic contribution similar to Eq. 18

$$P_\alpha = \hat{P}_\alpha + \frac{\Delta \bar{P}_\alpha x}{\rho_\alpha g \ell}, \quad \alpha = \beta,\gamma \tag{66}$$

The periodicity conditions are

$$v_\alpha(x) = v_\alpha(x \pm n), \quad \alpha = \beta,\gamma \tag{67}$$

$$\hat{P}_\alpha(x) = \hat{P}_\alpha(x \pm n), \quad \alpha = \beta,\gamma \tag{68}$$

and

$$r_\beta(x) = r_\beta(x \pm n) \tag{69}$$

The dimensionless pressure drop of each phase including gravitational contributions is given by

$$\psi_\alpha = 1 - \frac{\Delta\bar{P}_\alpha}{\rho_\alpha g \ell}, \quad \alpha = \beta,\gamma \tag{70}$$

For a given gas-liquid system and a given tube geometry, the system of equations stated above is completely determined (up to an arbitrary constant for the $\hat{P}$ fields) when two parameters are specified: the pressure drop of one of the phases (ψ_β or ψ_γ), and a boundary value of the gas-liquid interface location, for instance, r_β at $x = 0$. Note that the mean pressure drops $\Delta\bar{P}$ for each phase are equal; however, $\psi_\beta \neq \psi_\gamma$ because of the difference in density between liquid and gas.

Let us now consider the case in which there is no net flow of gas phase, i.e., the gas is stagnant and the liquid flows downward under the effect of gravity. Under these conditions the pressure in the gas phase is a constant and, since the system of equations stated above depends on pressure differences and pressure gradients, we can set a zero level of pressure for P_γ,

$$P_\gamma = 0 \tag{71}$$

In this case, the motion of the gas phase will only be that induced by the velocity of the liquid at the free surface, according to Eq. 49. It can be shown (Sáez, 1984) that if the following constraint is satisfied, the tangential stresses of the gas are negligible in Eq. 53.

$$\left(\frac{r_\sigma}{r_\beta} - 1\right)\frac{\mu_\gamma}{\mu_\beta} \ll 1 \tag{72}$$

For most gas-liquid systems, the viscosity ratio μ_γ/μ_β is much lower than one. Under these conditions, the hydrodynamics of the gas phase is completely decoupled from what occurs in the liquid phase. The problem is reduced to the following set of equations,

$$\nabla \cdot v_\beta = 0 \quad r_\beta \le r \le r_\sigma \tag{73}$$

$$-\nabla P_\beta + e_x + \nabla \cdot \tau_\beta = 0 \quad r_\beta \le r \le r_\sigma \tag{74}$$

$$v_\beta = 0 \quad \text{at } r = r_\sigma \tag{75}$$

$$v_\beta \cdot n_{\beta\gamma} = 0 \quad \text{at } r = r_\beta \tag{76}$$

$$\left(P_\beta + \frac{2H}{E\ddot{o}}\right)n_{\beta\gamma} = \tau_\beta \cdot n_{\beta\gamma} \quad \text{at } r = r_\beta \tag{77}$$

$$v_\beta(x) = v_\beta(x \pm n) \tag{78}$$

$$P_\beta(x) = P_\beta(x \pm n) \tag{79}$$

$$r_\beta(x) = r_\beta(x \pm n) \tag{80}$$

For a given gas-liquid system (fixed $E\ddot{o}$) and a given geometry [fixed $r_\sigma(x)$], the system of equations stated above is closed when a boundary value for $r_\beta(x)$ is specified.

We will now consider the calculation of macroscopic parameters. One of the most important macroscopic manifestations of the two-phase flow phenomenon is the liquid saturation, S_β, defined as the ratio of the volume occupied by the liquid phase to the total void volume. The liquid saturation can be calculated, after $r_\beta(x)$ has been determined, by the equation

$$S_\beta = \frac{\int_0^1 (r_\sigma^2 - r_\beta^2)\,dx}{\int_0^1 r_\sigma^2\,dx} \tag{81}$$

The liquid phase relative permeability is determined by means of Eq. 9.

The one-phase flow pressure drop is given by Eq. 41. The two-phase flow dimensionless pressure drop is defined by Eq. 70. For the case being considered in Eqs. 73–80, the pressure drop in the gas phase is decoupled from the equations of motion for the liquid. As a result, the liquid phase pressure drop $\Delta\bar{P}_\beta = 0$. From Eq. 70 the value of $\psi_\beta = 1$. Eq. 9 then reduces to

$$k_\beta = \psi_\beta^{(1)} = A\frac{Re_\beta^*}{Ga_\beta^*} \tag{82}$$

where use has been made of Eq. 41. The Reynolds and Galileo numbers are computed at the interstitial velocity of the liquid. The definitions of Re_β^* and Ga_β^* are the same as in Eq. 40 with u replaced by

$$u_\beta = \frac{1}{V}\int_{V_\beta} v'_\beta dV \tag{83}$$

$$Re_\beta^* = \frac{\rho_\beta u_\beta d'_h}{\mu_\beta}; \quad Ga_\beta^* = \frac{\rho_\beta^2 g d'^3_h}{\mu_\beta^2} \tag{84}$$

Here V_β is the volume of liquid in the conduit, and V is the total volume available for flow in the conduit. When $V_\beta = V$ the conduit is filled with liquid and there is no gas present. From Eq. 56 we see that if we integrate both sides over V_β and divide by V and then use the definitions in Eq. 40 for the Reynolds and Galileo numbers we get

$$\frac{Re_\beta^*}{Ga_\beta^*} = \left[\frac{1}{V}\int_{V_\beta} v_{\beta x}\,dV\right]\frac{\ell^2}{d'^2_h} \tag{85}$$

The calculation of k_β then proceeds as follows. Equations 73–80 are solved for $v_{\beta x}$. Values of d'_h are obtained for a given shape of the conduit $r_\sigma(x)$ using Eq. 43. The results are substituted in Eq. 85. The value of A comes from the one-phase flow computations in Eq. 42, and k_β is calculated according to Eq. 82. Different liquid saturations are obtained, corresponding to different Reynolds and Galileo numbers for the liquid, by fixing different values for the boundary condition for $r_\beta(x)$, the interface shape.

The general two-phase flow problem, stated by Eqs. 44 to 69,

can be greatly simplified by considering the special case in which the velocity of the gas phase is small. If the forced motion of the gas phase is not enough to induce large normal stresses at the gas-liquid interface and appreciable pressure drops in the liquid phase, then the normal momentum balance (Eq. 53) reduces to Eq. 77 and the equations describing the hydrodynamics of both phases are decoupled. Under these conditions, Eqs. 73 to 80 are enough to determine the liquid phase velocity and pressure profiles, as well as the location of the gas-liquid interface. The equations describing the hydrodynamics of the gas phase for this particular case reduce to

$$\nabla \cdot \boldsymbol{v}_\gamma = 0 \quad 0 \le r \le r_\beta \tag{86}$$

$$-\nabla \hat{P}_\gamma + \psi_\gamma \boldsymbol{e}_x + \nabla \cdot \tau_\gamma = 0 \quad 0 \le r \le r_\beta \tag{87}$$

$$\boldsymbol{v}_\gamma = \boldsymbol{v}_\beta(\omega/\xi) \quad \text{at } r = r_\beta \tag{88}$$

$$\frac{\partial \boldsymbol{v}_\gamma}{\partial r} = 0 \quad \text{at } r = 0 \tag{89}$$

$$\boldsymbol{v}_\gamma(x) = \boldsymbol{v}_\gamma(x \pm n) \tag{90}$$

$$\hat{P}_\gamma(x) = \hat{P}_\gamma(x \pm n) \tag{91}$$

where we have decomposed P_γ into a periodic and a macroscopic contribution (see Eq. 18) and we have combined Eqs. 49 and 52 into a unique condition, Eq. 88. Once the solution of the liquid phase problem is obtained, Eqs. 86 to 91 can be solved for a prescribed value of the pressure drop ψ_γ. The gas phase Reynolds number corresponding to this pressure drop can then be calculated from an equation analogous to Eq. 84.

$$\frac{Re_\gamma^*}{Ga_\gamma^*} = \frac{1}{d_h^2}\frac{1}{V}\int_{V_\gamma} v_{\gamma x}\, dV \tag{92}$$

and the gas phase relative permeability can be determined from Eq. 9, for which $\psi_\gamma^{(1)}$ is previously evaluated from Eq. 38.

Straight Tube Model

The simplest conduit model consists of a straight capillary tube in which the wall profile is not a function of axial distance. In this case the equations governing the two-phase flow hydrodynamics (Eqs. 44 to 69) become one-dimensional and it is possible to find analytical solutions for the velocity profiles. By taking the interstitial averages of the velocity profiles and using the definitions of the corresponding dimensionless parameters, the following macroscopic equations are obtained

$$\frac{Re_\beta^*}{Ga_\beta^*} = \frac{\psi_\beta}{72}(1-\kappa^2)^2 - (1-\xi)\frac{\kappa^2}{18}\left[\frac{(1-\kappa^2)}{2} + \kappa^2 \ln \kappa\right] \tag{93}$$

$$\frac{Re_\gamma^*}{Ga_\gamma^*} = \frac{\psi_\gamma}{72}\kappa^4 + \frac{\omega\kappa^2}{18\xi}\left[\frac{\psi_\beta}{2}(1-\kappa^2) + (1-\xi)\kappa^2 \ln \kappa\right] \tag{94}$$

$$(1-\psi_\gamma)\xi = 1 - \psi_\beta \tag{95}$$

where

$$\kappa = \frac{r_\beta}{r_\sigma} = S_\gamma^{1/2} \tag{96}$$

The single-phase flow pressure drop is given in this case by the Hagen-Poiseuille equation

$$\psi_\alpha^{(1)} = 72\frac{Re_\alpha^*}{Ga_\alpha^*}, \quad \alpha = \beta,\gamma \tag{97}$$

where in this case the hydraulic diameter is three times the tube diameter. Eq. 97 is equivalent to assigning a value of 72 to the Ergun constant.

The relative permeability of each phase can now be evaluated from Eq. 9. After some manipulations, the liquid phase relative permeability can be expressed by

$$k_\beta = S_\beta^2 + \frac{2(1-\xi)(1-S_\beta)^2[S_\beta + (1-S_\beta)\ln(1-S_\beta)][1-S_\beta(1-2\omega)]}{(1-\xi)(1-S_\beta)^2[2\omega\ln(1-S_\beta)-1] - 72\,Re_\gamma^*/Ga_\gamma^*} \tag{98}$$

Figure 3 shows the $k_\beta - S_\beta$ curves calculated for the air-water system at 20°C ($\xi = 1.2 \times 10^{-3}$, $\omega = 0.019$). The most important conclusion to be drawn from this figure is the insensitivity of the relative permeability curves to the value of Re_γ^*/Ga_γ^*. In normal applications (Sáez and Carbonell, 1985), this parameter rarely becomes greater than 1. Larger values often imply that the system is in the pulsing regime. This result is consistent with the assumption made by Sáez and Carbonell that the liquid relative permeability is independent of the gas flow rate. This fact simplifies greatly the analysis of experimental data since it implies that the liquid phase relative permeabilities can be determined by performing measurements of liquid holdup under no gas flow conditions, as shown by Sáez and Carbonell.

The curves in Figure 3 are also relatively insensitive to changes in the viscosity and density ratios. When ω is changed from 0 to 0.1, which is the usual range for gas-liquid systems, almost no variations in k_β occur. The values reported for $\xi = 1.2 \times 10^{-3}$ are very close to those obtained for $\xi = 0$. This insen-

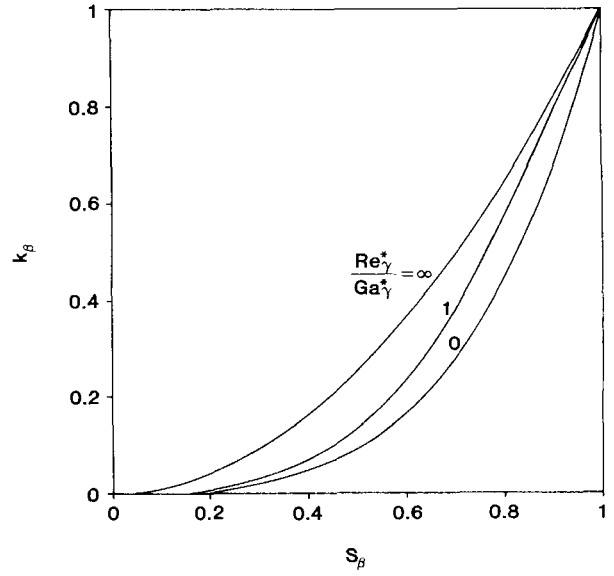

Figure 3. Liquid phase relative permeability, capillary tube model.

sitivity to ξ and ω implies that all effects of physical properties are accounted for in the basic dimensionless groups Re^* and Ga^*.

The gas phase relative permeability is given by

$$k_\gamma = S_\gamma\left\{\frac{\Omega[S_\gamma + 2\omega(1-S_\gamma)] + (1-\xi)S_\gamma(1-S_\gamma)^2(1-2\omega\ln S_\gamma)}{\Omega + (1-\xi)(1-S_\gamma)^2}\right\} \tag{99}$$

where

$$\Omega = -72\frac{Re^*_\beta}{Ga^*_\beta} - 2S_\gamma(1-\xi)(1-S_\gamma + S_\gamma\ln S_\gamma) \tag{100}$$

An equation similar to Eq. 99 can be obtained to express k_γ as a function of S_γ and Re^*_γ/Ga^*_γ.

The gas phase relative permeability curves are shown in Figure 4. The curves are shown in two different ways: curves at constant Re^*_γ/Ga^*_γ (solid lines) and curves at constant Re^*_β/Ga^*_β (dashed lines). An interesting phenomenon is observed when Re^*_β/Ga^*_β is held constant. At a specific saturation, which we will call the critical saturation, the relative permeability goes asymptotically to infinity. The value of S_γ at which this occurs can be computed by letting the denominator in Eq. 99 go to zero. It can be shown that this is also the point at which the pressure drop in the gas phase is only compensating the gravitational effects ($\psi_\gamma = 0$). Under these conditions, the velocity profile of the gas phase is uniform; i.e., the gas has everywhere a velocity equal to that of the liquid at the gas-liquid interface. The resulting gas flow rate is then just the effect of the drag that the liquid flow exerts on the gas. The critical saturation represents physically the lowest value of S_γ that can be achieved for a given Re^*_β/Ga^*_β so that there is no upward flow of gas. If the gas flow rate (or, rigorously speaking, Re^*_γ/Ga^*_γ) is increased beyond the value leading to the critical saturation, we move downward along the dashed lines in Figure 4. At first, the relative permeability decreases while the gas saturation remains practically constant, indicating that the gas flow rate is not high enough to exert forces at the gas-liquid interface that result in a change in the location of that boundary. As the gas flow rate is further increased, the gas saturation starts to increase, indicating a displacement of the gas-liquid interface toward the wall of the tube due to the forces exerted by the gas. The relative permeability curves then go through a minimum and, when the gas phase saturation gets to be more than 10 to 20% larger than the critical value, all the curves at constant Re^*_β/Ga^*_β coincide with

$$k_\gamma^{(ENV)} = S_\gamma^2 \tag{101}$$

This curve, which represents an envelope for all the relative permeability curves at Re^*_β/Ga^*_β constant, corresponds to the limit of k_γ as Re^*_γ/Ga^*_γ goes to infinity. This fact is well illustrated by the k_γ curves at constant Re^*_γ/Ga^*_γ, also shown in Figure 4.

When Sáez and Carbonell (1985) applied the relative permeability approach for the first time to the analysis of experimental data on pressure drops and liquid holdups in trickle beds, a single curve was found for the gas phase relative permeability, independent of gas and liquid Reynolds numbers (Eq. 8). However, that unique correlation was obtained from a limited amount of experimental data and it showed appreciable scatter. In a more recent work (Levec et al., 1984), a trend similar to that shown in Figure 4 was followed by experimentally determined relative permeabilities. In Part II we present an in-depth experimental study on the effect that the liquid and gas phase Reynolds numbers have on the gas phase relative permeabilities.

One of the disadvantages of the straight tube model is the fact that the surface tension forces play no role in the determination of holdups and pressure drops. The reason for this is that the straight tube model is based on a one-dimensional representation of the flow, thereby neglecting the effect that the curvature of the gas-liquid interface has on the characteristics of the flow. In order to account for surface tension forces, a model with a two- or three-dimensional representation of the pore spaces is required. This type of model is developed in the following section.

Periodically Constricted Tube Model

It has been empirically observed that complex unconsolidated porous media seem to have approximately the same functional relations for describing macroscopic parameters when an appropriate characteristic length, such as the hydraulic diameter, is chosen in the definition of the independent dimensionless variables. For instance, Sáez and Carbonell (1985) showed that the relative permeability-saturation curves were the same for packings of completely different shapes (spheres, cylinders, Raschig rings, etc.) when the hydraulic diameter of the packing was used in the definition of Reynolds and Galileo numbers. We can use this fact to suggest that a spatially periodic model based on a one-particle unit cell should give a fair estimate of those parameters. The simplest three-dimensional geometry that exhibits the spatial periodicity of such an elementary unit cell is a uniform cubic array of spheres. We will propose as the geometry of the model a periodically constricted tube that resembles the geometrical characteristics of the interstitial space of a cubic array of spheres.

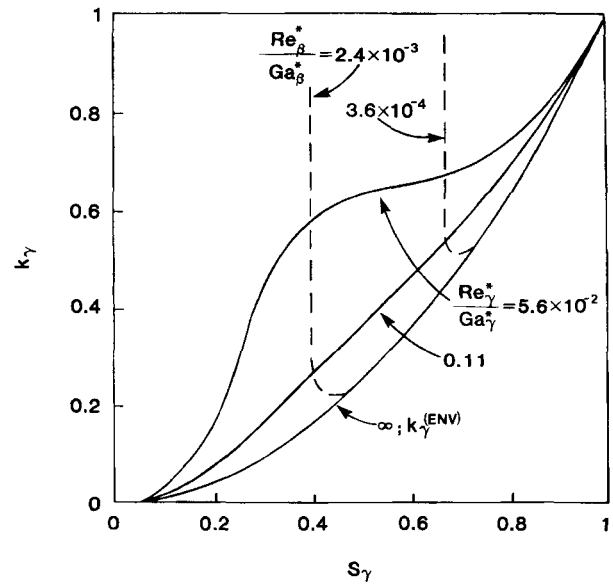

Figure 4. Gas phase relative permeability, capillary tube model.

Let us consider the case of macroscopic one-dimensional flow through a cubic array of spheres. Let x be the direction of macroscopic flow and consider for simplicity the length of the unit cell to be one. If we take successive cross sections of the flow path by cutting the structure with planes of constant x, we generate the flow path schematized in Figure 5. The solid lines represent the surface of the spheres and the dashed lines are symmetry planes. We have taken $x = 0$ to be the plane with the minimum area for flow (plane at which the spheres touch). Figure 5c represents the section with the maximum area available for flow. In the figure, the corners of the square are contact points between spheres.

Two important observations are obtained from the flow path depicted in Figure 5. First of all, the geometry is not axisymmetric but fully three-dimensional. Also, the surface delimiting the flow path consists of solid walls and symmetry planes. We will represent the flow path by means of a periodically constricted tube with the same cross-sectional area as a function of x as that of the cubic array of spheres. The use of an axisymmetric model implies that some geometrical characteristics are lost, but the mathematical complexity of the problem is greatly reduced. Another important consideration is that the symmetry planes are not solid surfaces. However, the velocity component normal to those planes is zero owing to the symmetry of the flow. The other components are expected to be small in any case due to the fact that the symmetry surfaces are closed (they have the same shape as the surface represented in Figure 5a). This implies, along with symmetry considerations, that there is no net flow across any closed line on those surfaces, so that the only possible motion of the fluid would be following symmetric recirculation patterns. If we consider that the velocity at the symmetry surfaces is negligible, then the only difference between symmetry planes and solid surfaces is that the normal stresses are zero in the former. The normal stresses at the wall of a periodically constricted tube are relatively small in the expanding region of the flow (Sáez, 1984), which coincides with the predominance of the symmetry surfaces in the flow path of the cubic array of spheres. The preceding analysis does not provide a formal justification for the use of the periodically constricted tube model, but it gives an intuitive appeal to such a representation.

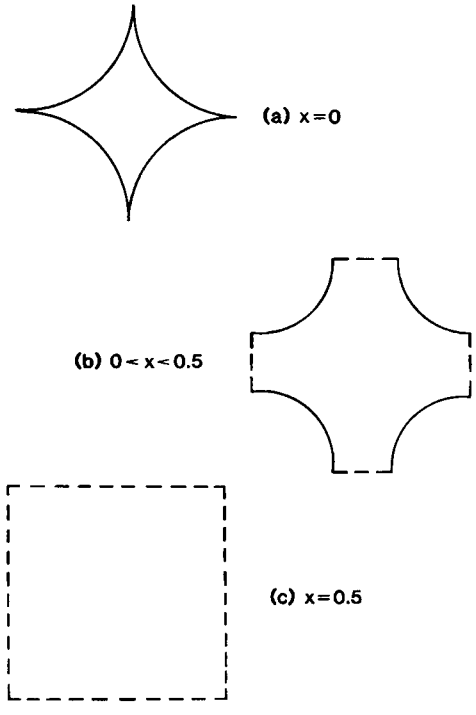

Figure 5. Flow path through a cubic array of spheres.

The cross-sectional area of the cubic array flow path as a function of x can be found by simple geometrical considerations. The result is

$$A(x) = \begin{cases} 1 - \pi/4 + \pi x^2 & 0 \le x \le 0.5 \\ 1 - \pi/4 + \pi(1-x)^2 & 0.5 \le x \le 1 \end{cases}$$

The periodically constricted tube will have the same area, so that its wall profile can be found by means of

$$\pi r_\sigma^2(x) = A(x)$$

The result is

$$r_\sigma(x) = \begin{cases} \left[\frac{1}{\pi} - \frac{1}{4} + x^2\right]^{1/2} & 0 \le x \le 0.5 \\ \left[\frac{1}{\pi} - \frac{1}{4} + (1-x)^2\right]^{1/2} & 0.5 \le x \le 1 \end{cases} \tag{102}$$

Now that the geometry is fixed, one solution to the fundamental equations (Eqs. 28 to 34) is enough to provide the general solution for the case of one-phase flow through the model geometry (Eq. 102), according to our formulation.

The problem was solved by means of finite-element methods. The solution was formulated in terms of biquadratic approximating functions for the velocity vector and bilinear functions for the pressure field. Eight-node quadrilateral elements were found to be the most stable elements for that type of approximation scheme. Details of the formulation and solution are given by Sáez (1984).

The solution to the one-phase flow problem yields an Ergun constant of $A = 125$. This value is 20% lower than the calculated value of 157 obtained by Sørensen and Stewart (1984a) and Zick and Homsy (1982) by solving the one-phase flow problem in a cubic array of spheres. However, in beds of spheres packed in a "uniformly ramdom" manner (Macdonald et al., 1979) the value of A corresponding to a bed with the porosity of a cubic array of spheres ($\epsilon = 0.48$) is 136, which is only 9% higher than $A = 125$. In any case, errors of less than 20% are inside the range of approximation of the Ergun equation so that the model proposed in this work can be considered adequate.

Let us now consider the case of free surface flow through the model geometry, i.e., the liquid flows along the walls of the tube and the gas phase is stagnant and occupies the core region. The formulation of the problem is given by Eqs. 73 to 80. The solution to this set of equations depends on two parameters: the Eötvös number, $E\ddot{o}$, and a boundary value of $r_\beta(x)$. When these two parameters were specified, it was determined numerically that the solution of the problem was unique and that there was a one-to-one correspondence between the boundary value of r_β and the dimensionless group Re_β^*/Ga_β^*, obtained from the solution by means of Eq. 85 (Sáez, 1984). According to this, we can state

that the solution of the problem is determined by $E\ddot{o}$ and Re^*_β/Ga^*_β. Therefore, the liquid saturation, S_β, can be expressed as

$$S_\beta = S_\beta(E\ddot{o}, Re^*_\beta/Ga^*_\beta) \tag{103}$$

Similar considerations lead to

$$k_\beta = k_\beta(S_\beta, E\ddot{o}) \tag{104}$$

Equation 104 states that the relative permeability-saturation curves are only functions of the Eötvös number.

The free surface flow problem consists of two linear differential equations (Eqs. 73 and 74) with nonlinear boundary conditions (Eqs. 75 to 80). The nonlinearity of the problem is due to the fact that the location of the free surface, $r_\beta(x)$, is unknown a priori. An iterative procedure was used to solve the problem. First, a location of the gas-liquid interface was assumed. Then, the linear problem consisting of Eqs. 72 to 75 and 77 to 80 was solved by means of the finite-element method. Once the velocity profiles were determined, Eq. 76 was used to generate a new interface shape and the procedure was repeated until convergence was achieved. The kinemetic condition (Eq. 76) is often used as the equation governing the iterative procedure in the literature on free surface flow problems (Nickell et al., 1974). This iterative scheme yielded a convergent solution when surface tension effects were not very large ($E\ddot{o} > 2$). For low Eötvös numbers, a different scheme was used. This scheme consisted of a direct search minimization of the variations of liquid flow rate

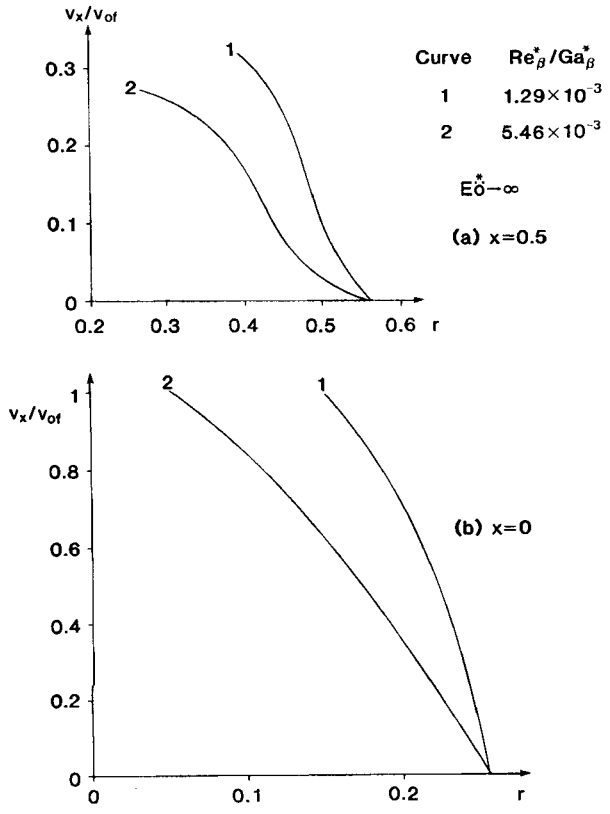

Figure 6. Axial velocity profiles of the liquid. Free surface flow through the model geometry, no surface tension effects.

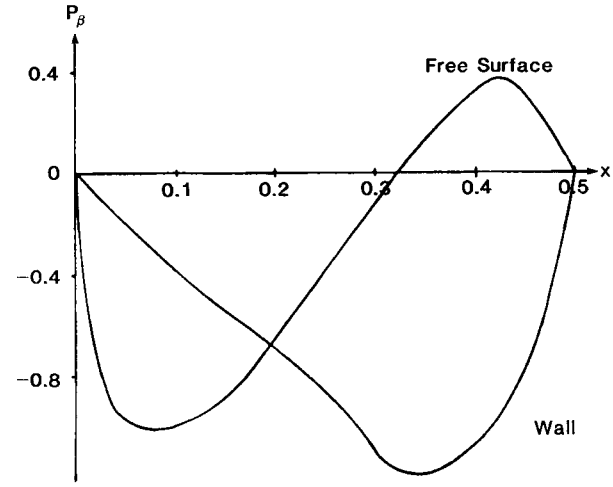

Figure 7. Pressure profiles in the liquid phase. Free surface flow through the model geometry; $E\ddot{o}^* \to \infty$, $Re^*_\beta/Ga^*_\beta = 5.46 \times 10^{-3}$.

as a function of x. The uniformity of liquid flow rates replaces Eq. 76 as the constraint for convergence. More details regarding the numerical solution are provided by Sáez (1984).

Typical axial velocity profiles for the free-surface flow problem are presented in Figure 6 for two different Re^*_β/Ga^*_β and two different axial locations ($x = 0$ corresponds to the point of constriction, whereas $x = 0.5$ corresponds to the point of expansion). Notice how the velocity profiles at $x = 0.5$ have an inflection point and show a trend toward smaller derivatives close to the wall of the tube ($r = 0.56$). This effect becomes more drastic for tubes with a large expansion radius. A recirculation region is sometimes observed in sinusoidal tubes with large amplitudes in

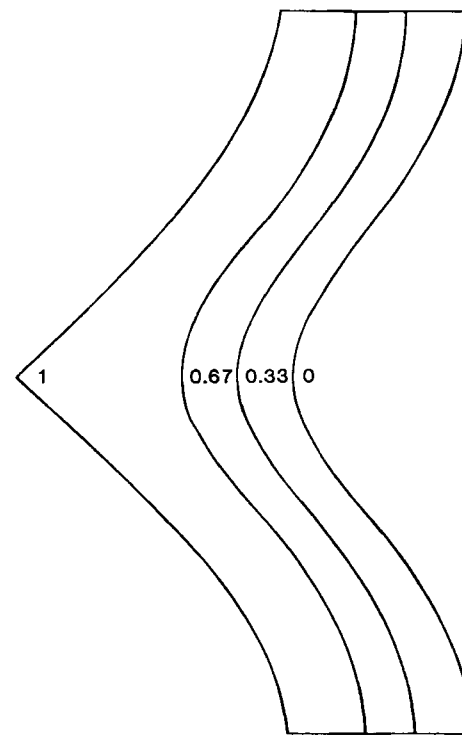

Figure 8. Streamlines; $E\ddot{o}^* \to \infty$, $Re^*_\beta/Ga^*_\beta = 5.46 \times 10^{-3}$.

the wall profile (Sáez, 1984). Pressure profiles are shown in Figure 7. They are presented for x between 0 and 0.5 since P_β is skewsymmetric about $x = 0.5$ for the case under consideration ($E\ddot{o} \rightarrow \infty$), as shown by Sáez (1984). The streamlines corresponding to this case are shown in Figure 8. The value assigned to each streamline corresponds to the fraction of the flow rate passing between the streamline and the free surface. The symmetry of the flow about the midpoint of the unit cell is easily observed in Figure 8. The streamlines are almost parallel in the region close to the free surface and a zone of low velocity is observed close to the wall. The results presented in Figures 6, 7, and 8 correspond to the particular case in which surface tension forces are zero ($E\ddot{o} \rightarrow \infty$). When surface tension effects are present, the symmetry of the flow is distorted by the presence of the term $2H\, n_{\beta\gamma}/E\ddot{o}$ in Eq. 77. Figures 9 and 10 show the axial velocity profiles and the streamlines corresponding to a low Eötvös number. Notice the gradual way in which the streamlines adopt the symmetric pattern of the wall profile, starting from a highly nonsymmetric free surface. The change in free surface shapes due to surface tension forces is better illustrated by Figure 11. In this figure the boundary value of $r_\beta(x)$ at $x = 0$ and 1 is held constant and the Eötvös number is changed. The interface evolves from a symmetric shape (*1*) to an almost flat shape (*3*). An increase in surface tension forces results in two effects: First, as $E\ddot{o}$ decreases, the interface becomes flatter (less curvature); second, the point of maximum radius is shifted from $x = 0.5$ at $E\ddot{o} \rightarrow \infty$ to lower values of x (upstream). This shift in the location of the interface was also observed by Dassori et al. (1984), who performed a perturbation solution of the two-phase

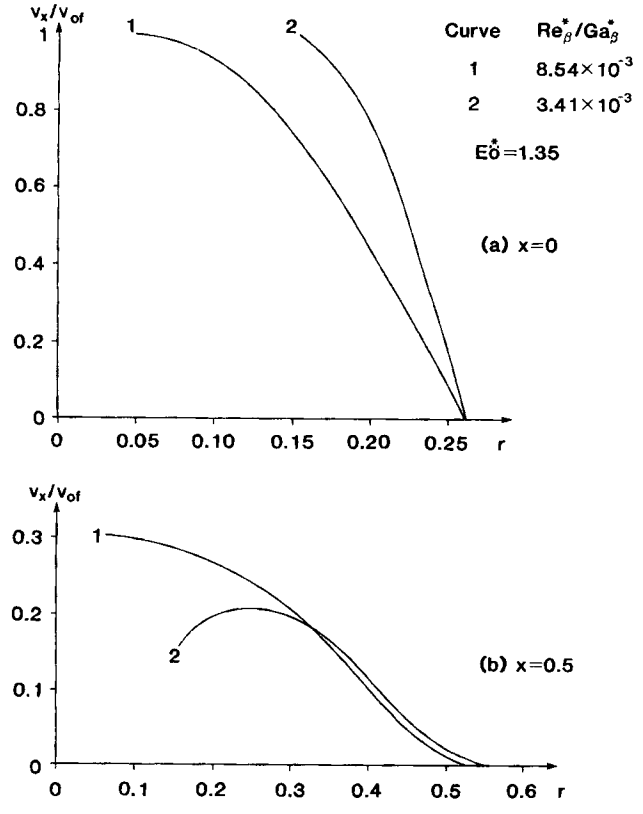

Figure 9. Axial velocity profiles of the liquid. Free surface flow through the model geometry, surface tension effects.

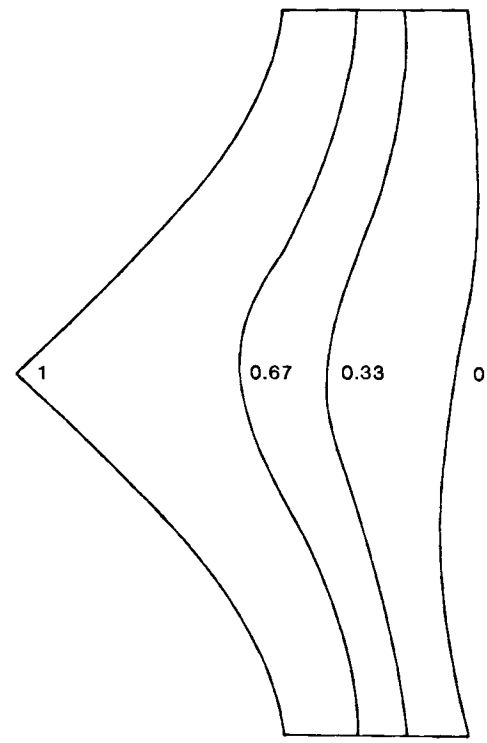

Figure 10. Streamlines; $E\ddot{o}^* = 1.35$, $Re^*_\beta/Ga^*_\beta = 8.54 \times 10^{-3}$.

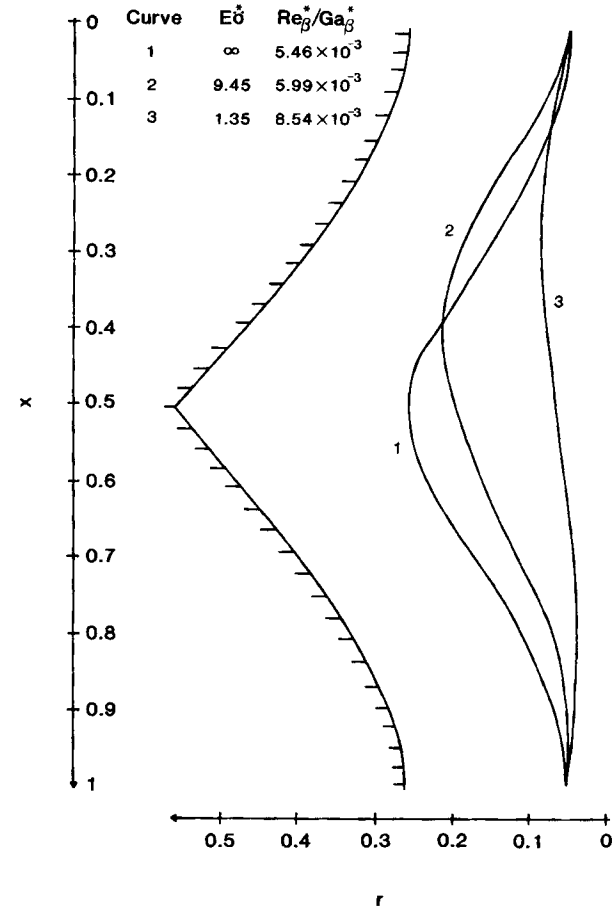

Figure 11. Interface shapes, surface tension effects.

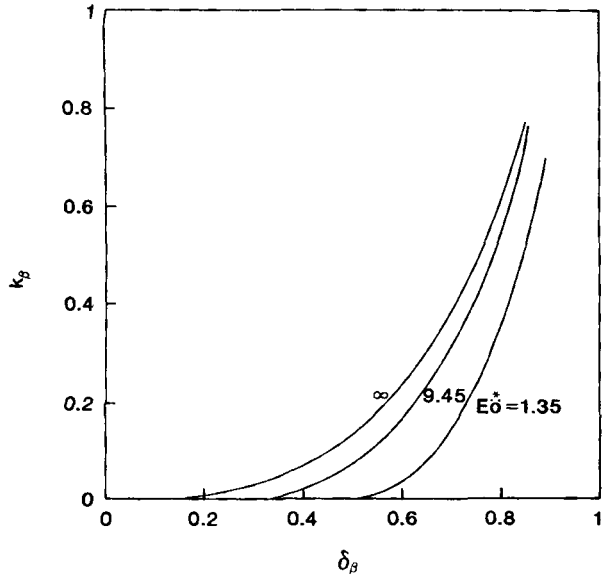

Figure 12. Liquid phase relative permeability, periodically constricted tube model.

flow problem in sinusoidal channels with small amplitudes in the wall oscillations.

The dramatic effect that surface tension forces have on the shape of the gas-liquid interface is manifested in the relative permeability curves, Figure 12, and in the direct prediction of liquid holdups, Figure 13. Sáez and Carbonell (1985) observed that the relative permeability curves of the liquid phase calculated from experimental data were insensitive to the Eötvös number in the range $0.1 < E\ddot{o}^* < 4$. These discrepancies might be a consequence of several factors that have not been taken into account in the present work. First of all, inertial effects have been neglected in the solution of the momentum equations. In a recent work, Gyure and Krantz (1983) showed that inertial effects were of extreme importance in the problem of free surface flow over a sphere. They point out that inertia results in a significant thinning of the liquid film thickness. This would be directly related to the retention of liquid on the particle surface. Another fact that could have appreciable importance is the instability of the flow in practical situations. The presence of waves and nonsteady phenomena at the surface of the liquid could affect the results of the model. Finally, we are always considering that the solid surface is completely wetted. This is probably not true in real situations. The consideration of partially wetted surfaces would introduce a great degree of complexity to the modeling process. Some empirical evidence of partial wetting is presented in Part II of this paper.

The gas phase relative permeabilities were estimated by considering the case in which the gas flow has no effect on the hydrodynamics of the liquid phase. Under these conditions, Eqs. 73 to 80 are used to describe the liquid phase hydrodynamics and Eqs. 86 to 91 are used to calculate gas phase pressure and velocity profiles. This approximation holds for low values of Re^*_γ/Ga^*_γ. The results obtained are shown in Figure 14 for a fixed Eötvös number. Notice that the approximation implies, in terms of relative permeability curves, that the $k_\gamma - S_\gamma$ curves at constant Re^*_β/Ga^*_β are vertical lines until they approach the envelope, which corresponds to the limit $Re^*_\gamma/Ga_{\gamma NE}{}^* \rightarrow \infty$. If we compare these results to the capillary tube model prediction (Figure 4), we notice that the approximation made only leads to noticeable errors in the region close to the envelope, in which it fails to predict the curvature of the k_γ curves. However, this failure implies very small errors in terms of relative permeability values so that the curves in Figure 14 are acceptable for practical purposes. The great simplification of the solution to the two-phase flow problem by making the no-interaction approximation makes this approach very practical.

The results presented in Figure 14, corresponding to no surface tension effects, do not differ very much with those given by the capillary tube model (Figure 4), although in general the constricted tube model gives lower values for k_γ. However, surface tension forces result in very large changes in the gas phase relative permeability curves, as shown in Figure 15.

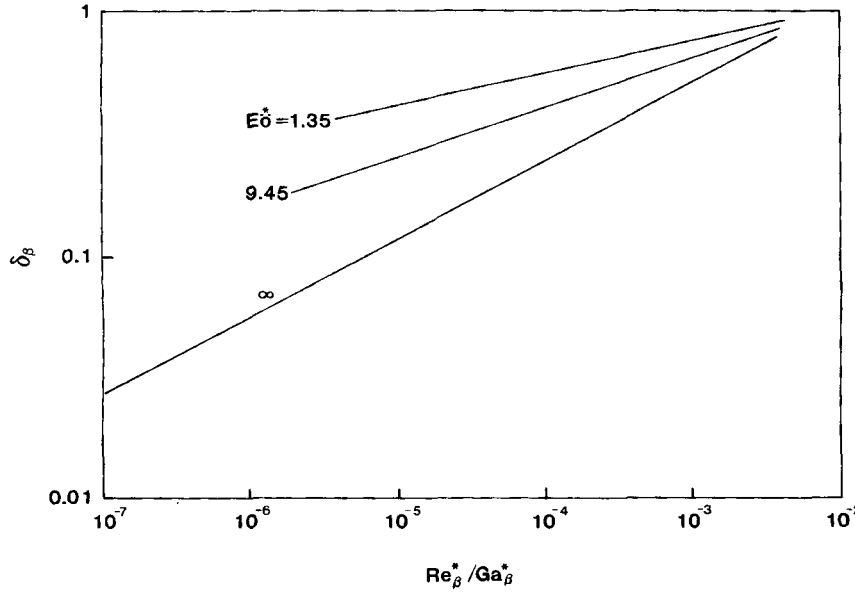

Figure 13. Reduced saturation dependence on $E\ddot{o}^*$ and Re^*_β/Ga^*_β, periodically constricted tube model.

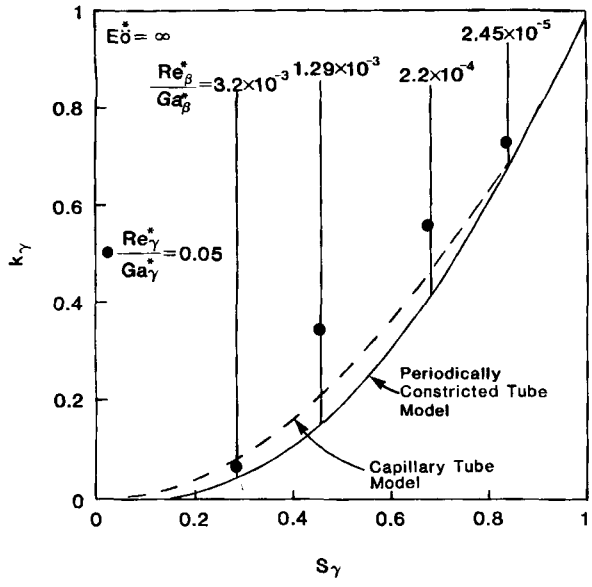

Figure 14. Gas phase relative permeability, periodically constricted tube model.

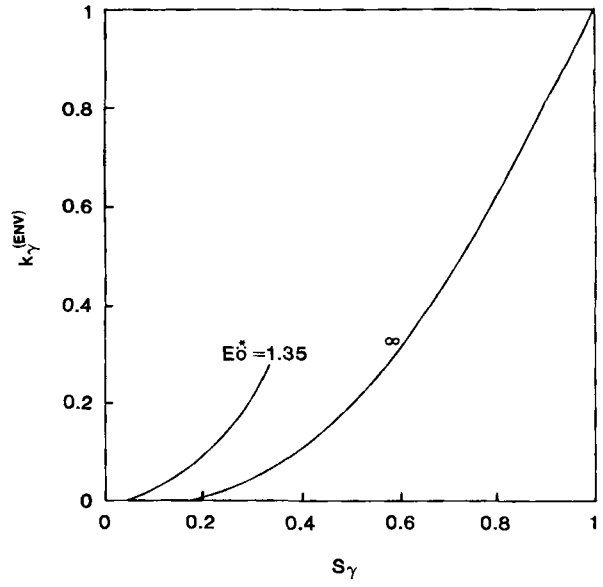

Figure 15. Effect of *Eö on envelopes of the gas phase relative permeability curves, periodically constricted tube model.**

The results presented above provide a complete physical representation of the trends followed by macroscopic parameters in stable two-phase flow through conduits. The physical insights obtained, in terms of the relative permeability analysis, present a basis for the study of the hydrodynamics of gas-liquid flows through packed beds. In Part II of this work we apply these results to the analysis of experimental data.

Acknowledgment

This work was supported in part by Chevron Research. A.E. Sáez is grateful to the Centro de Formación y Adiestramiento Petrolero y Petroquímico of Venezuela for financial support. J. Levec wishes to acknowledge financial aid from the Slovenian Research Council.

Notation

A = constant in the viscous terms of the Ergun equation
A_T = cross-sectional area of the conduit
A_w = internal area of the tube wall
B = constant in the inertial term of the Ergun equation
d'_h = hydraulic diameter, Eq. 39
$Eö$ = Eötvös number, Eq. 60
$Eö^*$ = Eötvös number based on the hydraulic diameter, = $Eö\,(d'^2_h/\ell^2)$
e_x = unit vector in the axial direction
g = acceleration of gravity
Ga^*_α = Galileo number of the α phase, based on the hydraulic diameter, $\rho^2_\alpha g d'^3_h/\mu^2_\alpha$
H = mean curvature of the gas-liquid interface, Eq. 61
k_α = relative permeability of the α phase
$k_\gamma^{(ENV)}$ = envelope of the gas phase relative permeability curves
ℓ = length of the unit cell
$n_{\beta\gamma}$ = unit vector normal to the gas-liquid interface, Eq. 64
P = pressure
$\overline{P}$ = area-averaged pressure, Eq. 21
$\tilde{P}$ = periodic part of the pressure field
$\Delta\mathcal{P}'$ = pressure drop, including gravitational contributions, Eq. 23
r = radial coordinate
Re^*_α = Reynolds number of the α phase, based on the hydraulic diameter, $\rho_\alpha u_\alpha d'_h/\mu$
r_s, r_c = principal radii of curvature, Eqs. 63 and 62, respectively
r_β = radial coordinate of the gas-liquid interface
r_σ = radial coordinate of the wall of the conduit
S_α = saturation of the α phase, Eq. 6
u = interstitial velocity, volumetric flow rate divided by column area
u_α = interstitial velocity of the α phase
v = velocity
V = volume available for fluid flow in a unit cell
v_{of} = velocity at $x = 0$, free surface
x = axial coordinate

Greek letters

δ_α = reduced saturation of the α phase, Eq. 5
ϵ = porosity
ϵ_β = liquid holdup per unit volume of bed
ϵ^o_β = static liquid holdup
$\lambda_{\beta\gamma}$ = unit rector tangent to the gas-liquid interface, Eq. 65
μ = viscosity
ξ = gas-to-liquid density ratio
ρ = density
σ = surface tension
τ = stres tensor
ψ_α = dimensionless pressure drop of the α phase, Eq. 35
$\psi^{(1)}_\alpha$ = dimensionless pressure drop of the α phase under one-phase flow conditions
ω = gas-to-liquid viscosity ratio

Subscripts

β = liquid phase
γ = gas phase

Special symbols

$'$ = variables with dimensions
$\langle\ \rangle$ = phase average
$\langle\ \rangle^\alpha$ = intrinsic phase average, = $\langle\ \rangle/\epsilon_\alpha$

Literature Cited

Adamson, A. W., *Physical Chemistry of Surfaces*, 3rd ed., Wiley, New York (1976).
Azzam, M. I. S., and F. A. L. Dullien, "Flow in Tubes with Periodic Step Changes in Diameter: A Numerical Solution," *Chem. Eng. Sci.*, **32**, 1,445 (1977).

Brenner, H., "Dispersion Resulting from Flow through Spatially Periodic Porous Media," *Phil. Trans. Royal Soc. London,* **297,** 81 (1980).

Carbonell, R. G., and S. Whitaker, "Heat and Mass Transport in Porous Media," in *Fundamentals of Transport in Porous Media,* J. Bear and Y. Corapcioglu, eds., Martinus Nijhoff, BV, The Netherlands, 121 (1984).

Dassori, C. G., J. A. Deiber, and A. E. Cassano, "Slow Two-Phase Flow through a Sinusoidal Channel," *Int. J. of Mult. Flow,* **10,** 181 (1984).

Deiber, J. A., and W. R. Schowalter, "Flow through Tubes with Sinusoidal Axial Variations in Diameter," *AIChE J.,* **25,** 638 (1979).

Eidsath, A. B., et al., "Dispersion in Pulsed Systems. III: Comparison between Theory and Experiments for Packed Beds," *Chem. Eng. Sci.,* **38,** 1,803 (1983).

Gianetto, A., et al., "Hydrodynamics and Solid-Liquid Contacting Effectiveness in Trickle-Bed Reactors," *AIChE J.,* **24,** 1,087 (1978).

Gyure, D. C., and W. B. Krantz, "Laminar Film Flow over a Sphere," *Ind. Eng. Chem. Fund.,* **22,** 405 (1983).

Levec, J., A. E. Sáez, and R. G. Carbonell, "Holdup and Pressure Drop in Trickle Bed Reactors," *Inst. Chem. Eng. Symp. Ser.* **87,** (1984).

Macdonald, I. F., et al., "Flow Through Porous Media—The Ergun Equation Revisited," *Ind. Eng. Chem. Fund., 18, 199 (1979).*

Neira, N. A., and A. C. Payatakes, "Collocation Solution of Creeping Newtonian Flow through Periodically Constricted Tubes with Piecewise Continuous Wall Profile," *AIChE J.,* **24,** 43 (1978).

———, "Collocation Solution of Creeping Newtonian Flow through Sinusoidal Tubes," *AIChE J.,* **25,** 725 (1979).

Nickell, R. E., R. I. Tanner, and B. Caswell, "The Solution of Viscous Incompressible Jet and Free-Surface Flows Using Finite-Element Methods," *J. Fluid Mech.,* **65,** 189 (1974).

Payatakes, A. C., C. Tien, and R. M. Turien, "A New Model for Granular Porous Media. I, II," *AIChE J.,* **19,** 58 (1973).

Payatakes, A. C., and M. A. Neira, "Model of the Constricted Unit Cell Type for Isotropic Granular Porous Media," *AIChE J.,* **23,** 922 (1977).

Pendse, H., H. W. Chiang, and C. Tien, "Analysis of Transport Processes with Granular Media Using the Constricted Tube Model," *Chem. Eng. Sci.,* **38,** 1,137 (1983).

Sáez, A. E., "Hydrodynamics and Lateral Thermal Dispersion for Gas-Liquid Cocurrent Flow in Packed Beds," Ph.D. Diss. Dept. Chem. Eng., Univ. California, Davis (1984).

Sáez, A. E., and R. G. Carbonell, "Hydrodynamic Parameters for Gas-Liquid Cocurrent Flow in Packed Beds," *AIChE J.,* **31** (1), 52 (1985).

Scheidegger, A. E., *The Physics of Flow Through Porous Media,* Univ. Toronto Press (1974).

Shah, Y. T., *Gas-Liquid-Solid Reactor Design,* McGraw-Hill, New York (1979).

Sørensen, J. P., and W. E. Stewart, "Computation of Forced Convection in Slow Flow Through Ducts and Packed Beds. II: Velocity Profile in a Simple Cubic Array of Spheres," *Chem. Eng. Sci.,* **29,** 819 (1974a).

———, "Computation of Forced Convection in Slow Flow Through Ducts and Packed Beds. III: Heat and Mass Transfer in a Simple Cubic Array of Spheres," *Chem. Eng. Sci.,* **29,** 827 (1974b).

Zanotti, F., and R. G. Carbonell, "Development of Transport Equations for Multiphase Systems. I, II, III," *Chem. Eng. Sci.,* **39,** 263 (1984).

Zick, A. A., and G. M. Homsy, "Stokes FLow through Periodic Arrays of Spheres," *J. Fluid Mech.,* **115,** 13 (1982).

Manuscript received Sept. 19, 1984, and revision received May 12, 1985.